Journal of Biomechanics 82 (2019) 116–123

Contents lists available at ScienceDirect

Journal of Biomechanics

journal homepage: www.elsevier.com/locate/jbiomech
www.JBiomech.com

Effects of lumbo-pelvic rhythm on trunk muscle forces and disc loads during forward flexion: A combined musculoskeletal and finite element simulation study

Tao Liu [a], Kinda Khalaf [b], Samer Adeeb [a], Marwan El-Rich [c,*]

[a] Department of Civil and Environmental Engineering, University of Alberta, Edmonton, Alberta, Canada
[b] Department of Biomedical Engineering, Khalifa University, Abu Dhabi, United Arab Emirates
[c] Department of Mechanical Engineering, Khalifa University, Abu Dhabi, United Arab Emirates

ARTICLE INFO

Article history:
Accepted 17 October 2018

Keywords:
Lumbo-pelvic rhythm
Finite element analysis
Musculoskeletal model
Flexion
Muscle forces
Load-sharing
Spinal load
Center of mass
Posture

ABSTRACT

Previous *in-vivo* studies suggest that the ratio of total lumbar rotation over pelvic rotation (lumbo-pelvic rhythm) during trunk sagittal movement is essential to evaluate spinal loads and discriminate between low back pain and asymptomatic population. Similarly, there is also evidence that the lumbo-pelvic rhythm is key for evaluation of realistic muscle and joint reaction forces and moments predicted by various computational musculoskeletal models. This study investigated the effects of three lumbo-pelvic rhythms defined based on *in-vivo* measurements on the spinal response during moderate forward flexion (60°) using a combined approach of musculoskeletal modeling of the upper body and finite element model of the lumbosacral spine. The muscle forces and joint loads predicted by the musculoskeletal model, together with the gravitational forces, were applied to the finite element model to compute the disc force and moment, intradiscal pressure, annular fibers strain, and load-sharing. The results revealed that a rhythm with high pelvic rotation and low lumbar flexion involves more global muscles and increases the role of the disc in resisting spinal loads, while its counterpart, with low pelvic rotation, recruits more local muscles and engages the ligaments to lower the disc loads. On the other hand, a normal rhythm that has balanced pelvic and lumbar rotations yields almost equal disc and ligament load-sharing and results in more balanced synergy between global and local muscles. The lumbo-pelvic rhythm has less effect on the intradiscal pressure and annular fibers strain. This work demonstrated that the spinal response during forward flexion is highly dependent on the lumbo-pelvic rhythm. It is therefore, essential to adapt this parameter instead of using the default values in musculoskeletal models for accurate prediction of muscle forces and joint reaction forces and moments. The findings provided by this work are expected to improve knowledge of spinal response during forward flexion, and are clinically relevant towards low back pain treatment and disc injury prevention.

1. Introduction

Forward flexion includes a combination of lumbar flexion and pelvic rotation, also referred to as, lumbo-pelvic coordination or rhythm (Granata and Sanford, 2000; Tafazzol et al., 2014). *In vivo* investigations, through measuring the kinematics of the lumbar spine (Arjmand and Shirazi-Adl, 2006; Granata and Sanford, 2000) and the lumbo-plevic rhythm during flexion, have demonstrated discrepancies in the variation of both rhythms in different experiments (Esola et al., 1996; Porter and Wilkinson, 1997; Tafazzol et al., 2014; Rose et al., 1988). Furthermore, the lumbo-pelvic rhythm was found different between healthy subjects and Low Back Pain (LBP) patients (Kim et al., 2013). A recent study revealed that the lumbar contribution to the lumbo-pelvic rhythm during flexion was about 22% smaller in chronic LBP patients as compared to control (Laird et al., 2016). Subjects with a history of LBP exhibited different lumbo-pelvic rhythms (Esola et al., 1996), yet reduced mobility (20%)of the pelvis as compared to asymptomatic subjects (Porter and Wilkinson, 1997), indicating that LBP can potentially be reduced by greater pelvic rotation. On the contrary, Vazirian et al. (2016) found that the magnitude of lumbar contribution decreases in LBP patients, the elderly and females, as well as with greater pace of motion, but increases with greater external load and back muscle fatigue.

* Corresponding author at: Department of Mechanical Engineering, Khalifa University, P.O. Box 127788, Abu Dhabi, United Arab Emirates.
E-mail address: marwan.elrich@ku.ac.ae (M. El-Rich).

https://doi.org/10.1016/j.jbiomech.2018.10.009
0021-9290/

Musculoskeletal (MSK) modeling, which allows the evaluation of muscle forces and joint reaction forces and moments, during forward flexion for instance requires accurate lumbar and pelvic rotation input for realistic predictions (Arjmand et al., 2011; Arjmand and Shirazi-Adl, 2006; Fathallah et al., 1999; Cholewicki and McGill, 1996). Arshad et al. (2016) reported that spine rhythms affects the shear and compression forces in the L4-5 disc as well as the global and local trunk muscle forces at maximum flexion position. Tafazzol et al. (2014) found that the lumbar spine contributed more to the trunk rotation during early forward flexion, while the pelvis contributed more during the final stage. The aforementioned research sheds light on the interactions between the lumbar spine and pelvic rotations and spinal forces. However, the effects of the lumbo-pelvic rhythm on load-sharing or intradiscal pressure (IDP) along the spine remain unknown.

This study, hence, aims to quantify the effects of three different lumbo-pelvic rhythms defined based on *in-vivo* data taken from the literature on the response of the lumbosacral spine during moderate forward flexion (up to 60°) using a combined MSK modelling and Finite Element (FE) analysis.

2. Methods

2.1. Musculoskeletal model

A previously-validated MSK model (Liu et al., 2018) was employed to calculate trunk local and global muscle forces during 60° forward flexion. The model was adjusted to average height and weight of 168 cm and 70 kg, respectively. The MSK model (version 6.0, AnyBody Technology A/S, Denmark) included the skull, upper arms, thorax, and lumbosacral spine. The lumbosacral spine L1-S1 included five rigid vertebrae (L1-5), five discs modeled as rigid joints with rotational degrees of freedom only and nonlinear flexural stiffness, seven ligaments, the sacrum, and the pelvis. The ligaments were simulated by springs for which the force is calculated as the product of the stiffness and length change during simulation. The facet joints were activated and the contact force was produced by detecting the distance between the contact points located between adjacent facet surfaces (Liu et al., 2018). The overall musculature of the MSK model included 188 muscle fascicles grouped into global and local muscles (Fig. 1). The muscles were modelled in the following three forms embedded in Anybody: a straight line connecting insertion and origin points, via-points muscles, and nonlinear wrapping muscles. Muscle strength was defined as the product of the maximum muscle stress to the physiological cross-sectional area (de Zee et al., 2007). Muscle forces were evaluated by minimizing the sum of the square of the ratios of muscle force and muscle strength (de Zee et al., 2007, Damsgaard et al., 2006). The MSK model also considered the intra-abdominal pressure (IAP), with magnitude fluctuating between 2.2 kPa and 4.4 kPa, during the simulations. The spine rhythm measured by Granata and Sanford (2000) was applied to the model as follows : 8% at T12-L1, 13% at L1-2, 16% at L2-3, 23% at L3-4, 26% at L4-5, and 14% at L5-S1. These percentages express the intersegmental rotations as a percentage of the total lumbar flexion.

2.2. Passive FE model

The 3D geometry of the L1-S1 bony structures was directly obtained from the MSK model, cleaned from spikes and sharp edges using Geomagic software (Geomagic Studio 2014), then meshed in Hypermesh (Hyperworks 14.0). The disc was created between two intervening endplates and divided into nucleus pulposus (NP) and annulus fibrosus (AF) reinforced by collagen fibers with nonlinear tension force-length relationship, with a volume ratio of 44% and 56%, respectively (El-Rich et al., 2009; Schmidt et al., 2006). The fibers were distributed in concentric lamellae with a crosswise pattern close to ±35° (El-Rich et al., 2009; Schmidt et al., 2007). A frictionless surface-to-surface contact

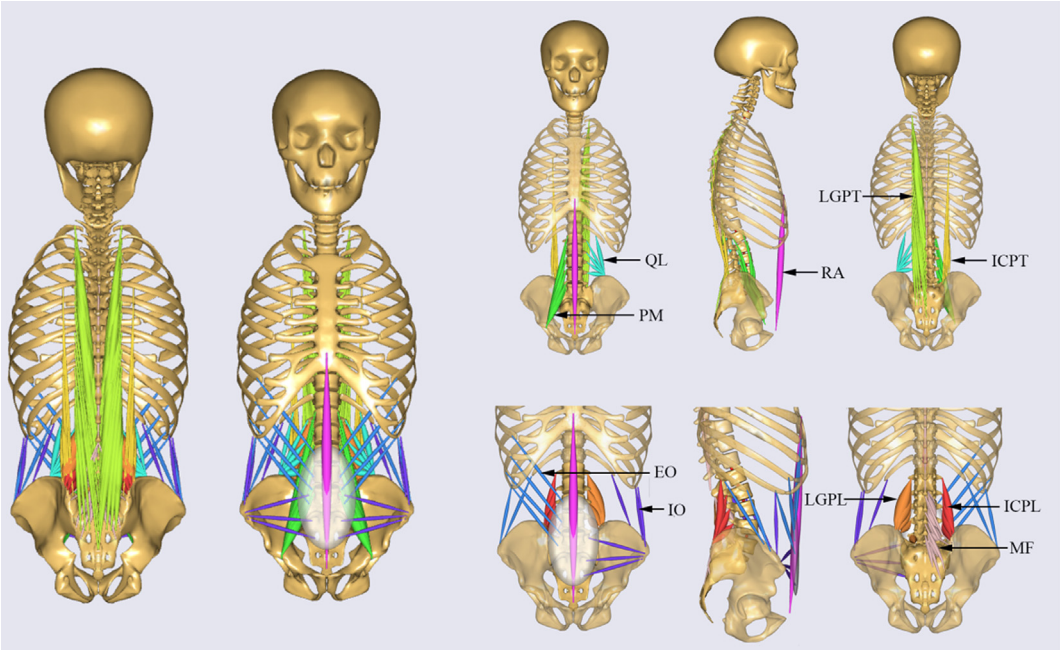

Fig. 1. Trunk muscle architecture in Anybody and individual muscle groups. Global muscles (1 Rectus Abdominis (RA), 12 Internal Oblique (IO), 12 External Oblique (EO), 16 Iliocostalis Lumborum Pars Thoracic (ICPT), 24 Longisimus Thoracis Pars Thoracic (LGPT)) and Local muscles (8 Iliocostalis Lumborum Pars Lumborum (ICPL), 10 Longisimus Thoracis Pars Lumborum (LGPL), 22 Psoas Major (PM), 38 Multifidus (MF) and 10 Quadratus Lumborum muscle fascicles (QL)) (Arshad et al., 2016).

was established between all facet joints with a minimal gap of 1.5 mm. The ligament force had the same force-length relationship and insertion points as those in the MSK model. The cartilaginous endplates and bones were assumed to be linear elastic while the annulus ground and NP were modeled using the hyper-elastic Mooney-Rivlin model. Details on material properties were provided elsewhere (Liu et al., 2018). All simulations were performed using Abaqus software (Abaqus 6.13-4). The sacrum was rotated based on the lumbo-pelvic ratios investigated in this study.

2.3. Load transfer from the MSK model to the FE model

The disc moment, ligament forces, and facet joint forces obtained at the level T12-L1 together with muscle forces at all levels of the MSK model were applied to the FE model. These loads resulted from the upper body weight and muscle forces and accounted for the IAP (Liu et al., 2018). To correct the small discrepancy in the deformed positions predicted by the MSK model and the FE model due to the difference in the modeling of the disc, the L1 vertebra was subjected to a slight anterior-posterior translation, in addition to the aforementioned loads. All muscle forces obtained from the MSK model were applied to the FE model at the insertion points as force vectors. The gravity force of each vertebra and the forces in the ligaments of the segment T12-L1 were applied as concentrated forces (Fig. 2).

2.4. Validation

The MSK model and passive FE model have been validated in our previous study (Liu et al., 2018). The MSK model was tested in neutral standing and flexion postures by comparing the compressive force in the joint L4-5 indirectly to the *in-vivo* measured IDP at the same level (Wilke et al., 2001). The FE model was also tested by comparing total rotation of L1 with respect to L5 produced by flexion and extension moments to other numerical (Dreischarf et al., 2014, Naserkhaki et al., 2016) and *in-vitro* (Rohlmann et al., 2001) data. The method of transferring the muscle forces from the MSK model to FE model, as well as simulation process, are also elaborated at length in our previous work (Liu et al., 2018).

2.5. Simulated tasks

Sixty degrees forward trunk flexion was simulated using three lumbo-pelvic rhythms as summarized in Table 1. These rhythms were defined based on the peak *in-vivo* ranges measured in previous studies (Rose et al., 1988; Esola et al., 1996; Porter and Wilkinson, 1997; Tafazzol et al., 2014).

3. Results

3.1. Posture and center of mass

The thorax and lumbar spine postures, as well the lever arms and the vertical positions of the gravity forces, varied with the lumbo-pelvic rhythm (Fig. 3). The center of mass (CoM) for the entire upper body was closer to the sacrum (217.9 mm) and was lower (60 mm) in the L20P40 model than in the other models. The L45P15 model, however, yielded posture with greater lever arms (221.4 mm) of the gravity forces and higher CoM (75 mm). The L36P24 model produced posture with greatest vertical distance of the CoM (77 mm). The reference frame of all CoMs is located at the posteriorly distal point of the sacrum.

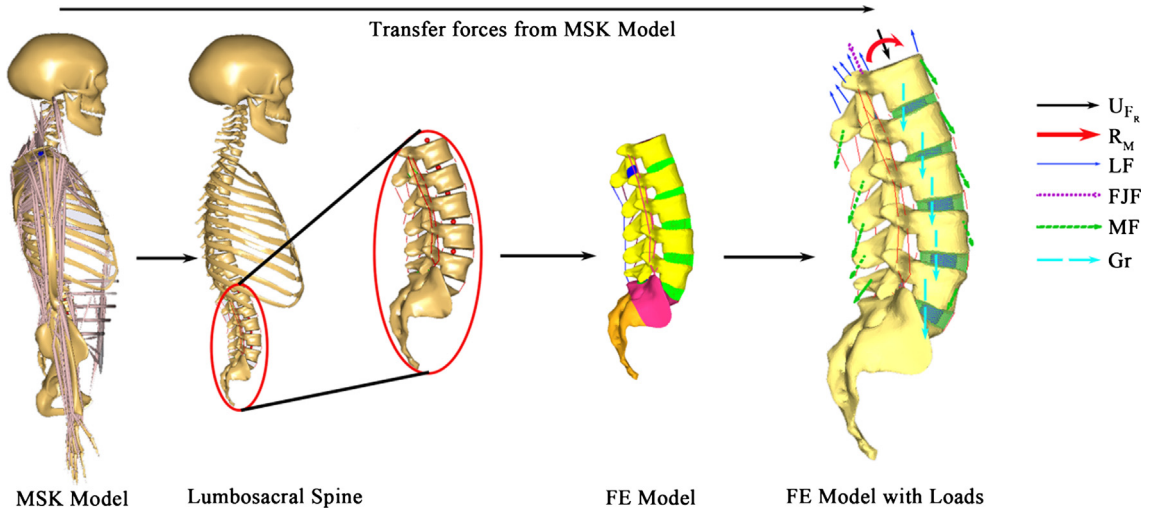

Fig. 2. The process of transferring forces from the MSK model to FE model. (U_{F_R}: Translation in the direction of the reaction force at T12-L1; R_M: Reaction moment at joint T12-L1; LF: Ligament forces; FJF: Facet joint forces; MF: Muscle forces; Gr: Gravitational force for each vertebra).

Table 1
The lumbo-pelvic rhythms applied to the model.

Lumbo-pelvic rhythm models*	Lumbar rotation angle/Pelvic rotation angle	Lumbar (L1-S1) rotation (°)	Pelvis rotation (°)
L20P40	0.5	20	40
L36P24	1.5	36	24
L45P15	3	45	15

* LnPm: n is the lumbar rotation, m is the pelvic rotation, n + m = 60° (total flexion rotation).

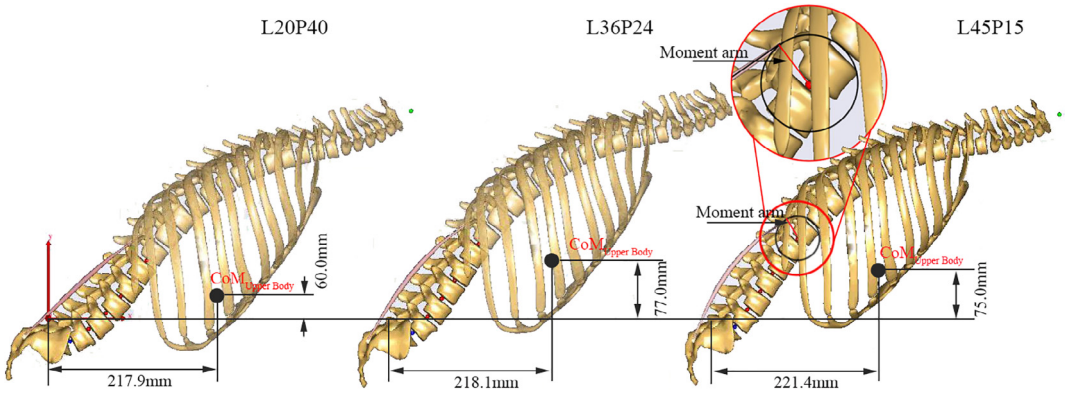

Fig. 3. Variation of posture and Center of Mass (CoM) of the upper body at 60° flexion with lumbo-pelvic rhythm.

3.2. Trunk muscle force

The total global and total local muscle forces were defined as the sum of all global and local muscle forces respectively (Fig. 4a). The total local muscle force increased almost linearly during the inclination of the upper body in all models. However, the total global muscle force fluctuated during the initial phrase of flexion and then increased during for the rest of the simulation. Both local and global muscle forces exhibited similar trends under the three different rhythms. The global muscle forces predicted by the L36P24 (moderate pelvic rotation) model exhibited the highest forces, followed by the L20P40 (high pelvic rotation) model, and finally by the L45P15 (low pelvic rotation) model during the initial 20°of flexion. Higher global muscle forces were found using the L20P40 model, followed by the L36P24 model. The L45P15 model came third in terms of the magnitude of global muscle forces from 20° to 55°, and then second during the last 5° of flexion, as it predicted slightly higher forces than the L36P24 model. Minor differences between the three models were observed in terms of the local muscle forces during the first 30° of the flexion. Although these differences increased during the last 30° flexion, the trend followed the same order (L45P15 > L36P24 > L20P40).

The forces for each muscle group were also predicted (Fig. 4b). The results demonstrate that the RA muscle and PM muscle group were silent throughout flexion for all rhythms. The L36P24 model was second in terms of group muscle force predictions, except for the ICPT muscle group. The muscle forces presented an ascending order in particular muscle groups (LGPL, QL, MF, IO, EO), and a descending order in the ICPL, LGPT groups as the lumbo-pelvic ratios varied from 0.5 to 3. The ICPT muscle force predicted by the L20P40 model presented the highest force value, followed by the muscle forces predicted by L45P15 model, and finally by the L36P24 model.

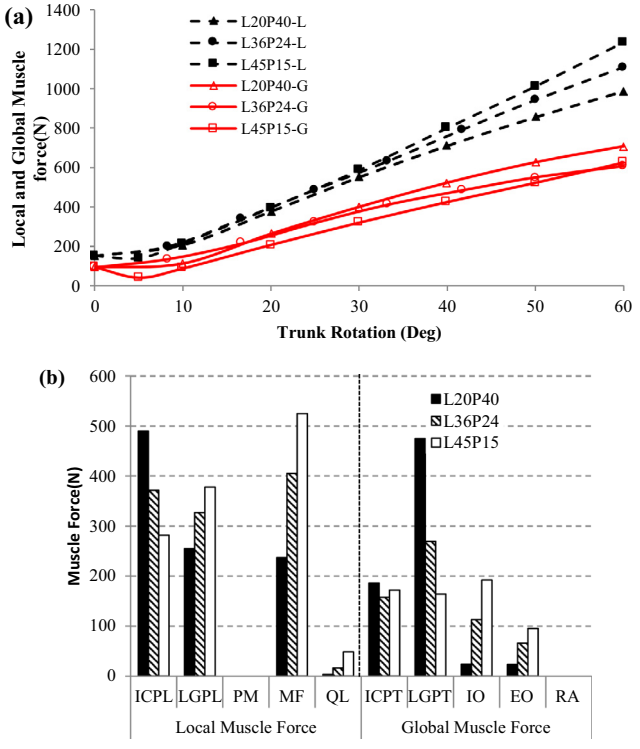

Fig. 4. (a) Variation of total local (L) and total global (G) muscle forces with lumbo-pelvic rhythms during 60° trunk forward flexion. (b) Variation of individual muscle group forces with lumbo-pelvic rhythm at 60° trunk forward flexion.

3.3. Disc strain

All three models predicted high tensile strains in the innermost area of the collagen fibres at the L2-S1 levels, but small tensile strains at the L1-2 level. For the L20P40 model, high tensile strain first appeared at the anterior area of the innermost lamella at the L2-5 level and then extended to the whole area of the innermost lamella at the L5-S1 level (Fig. 5). For the L36P24 model, high tensile strain was first detected at the anterior area of the innermost lamella at the L2-3 level and then transferred to the posterior area of the innermost lamella from L3 to L5, finally extending to the entire innermost lamella at the L5-S1 level. In the L40P15 model, the same trend occurred at the L2-5 levels similar to the L36P24 model. It should also be noted that as the lumbo-pelvic ratio was varied from 0.5 to 3, the proportions of the high tensile strain increased at the L2-5 levels, but decreased at the L5-S1 and L1-2 levels.

3.4. IDP

Overall, the L45P15 model predicted the highest IDP at all levels except the L5-S1. The maximum IDP difference was found between the L45P15 and the L20P40 models at the L4-5 level and reached ~15% (Fig. 6). The L20P40 and L36P24 models predicted almost the same IDP at the L1-3 and L5-S1 levels while the L20P40 model predicted the lowest IDP at the L3-5 levels.

3.5. Disc force and moment

The compressive force increased from the L1 to S1 levels for both the L20P40 and L36P24 models. The same trend was observed

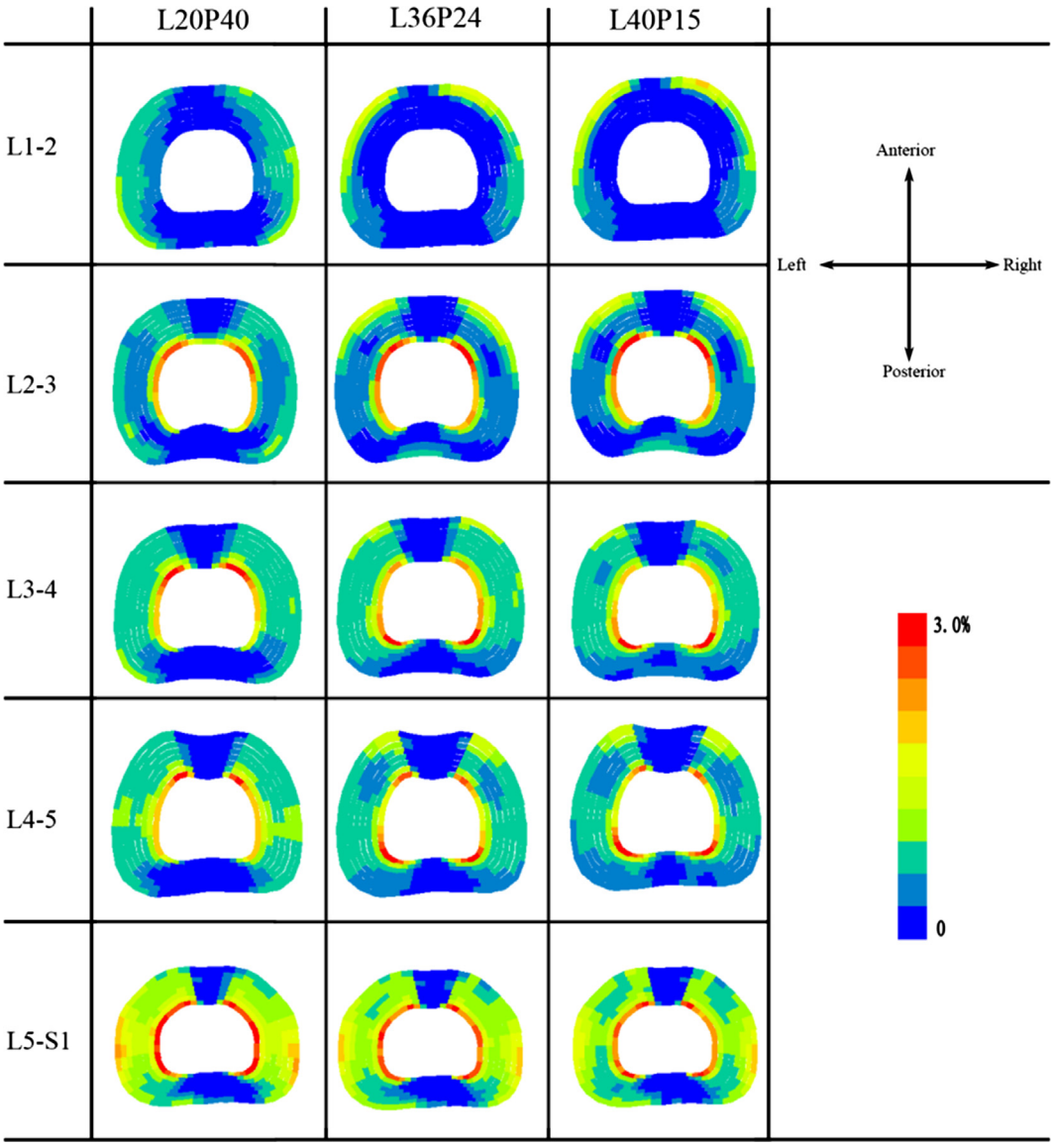

Fig. 5. Variation of annular fibers strain with lumbo-pelvic rhythm at 60° trunk forward flexion.

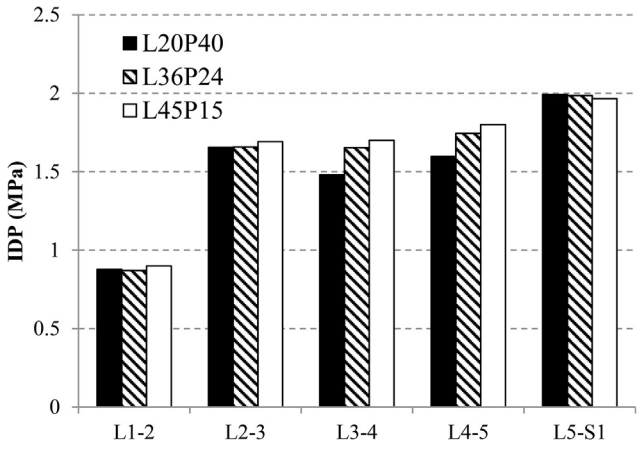

Fig. 6. Variation of IDP with lumbo-pelvic rhythm at 60° trunk forward flexion.

for the L45P15 model, except at the L3-4 level. The compressive force predicted by the L20P40 model was higher in comparison to the value predicted by L36P24 and L45P15 models at the L1-4 levels. The compressive force predicted by the L20P40 model was 115N greater than its counterpart from the L36P24 model, which was 47N greater than the compressive force predicted by the L45P15 model at the L3-4 level. However, the opposite pattern was observed at the L5-S1 level, where the maximum compression occurred in the L45P15 model and reached 1258N. The L20P40 and L36P24 models predicted similar compressive forces at the L4-5 levels, which were ~ 85N higher than the force predicted by the L45P15 model.

Shear forces demonstrated an increasing pattern from L1 to S1, where the maximum value was seen in the L20P40 model at 747N. The three models predicted anterior shear forces at all levels except the L20P40 model which predicted posterior shear force at the L1-2 level (Fig. 7a).

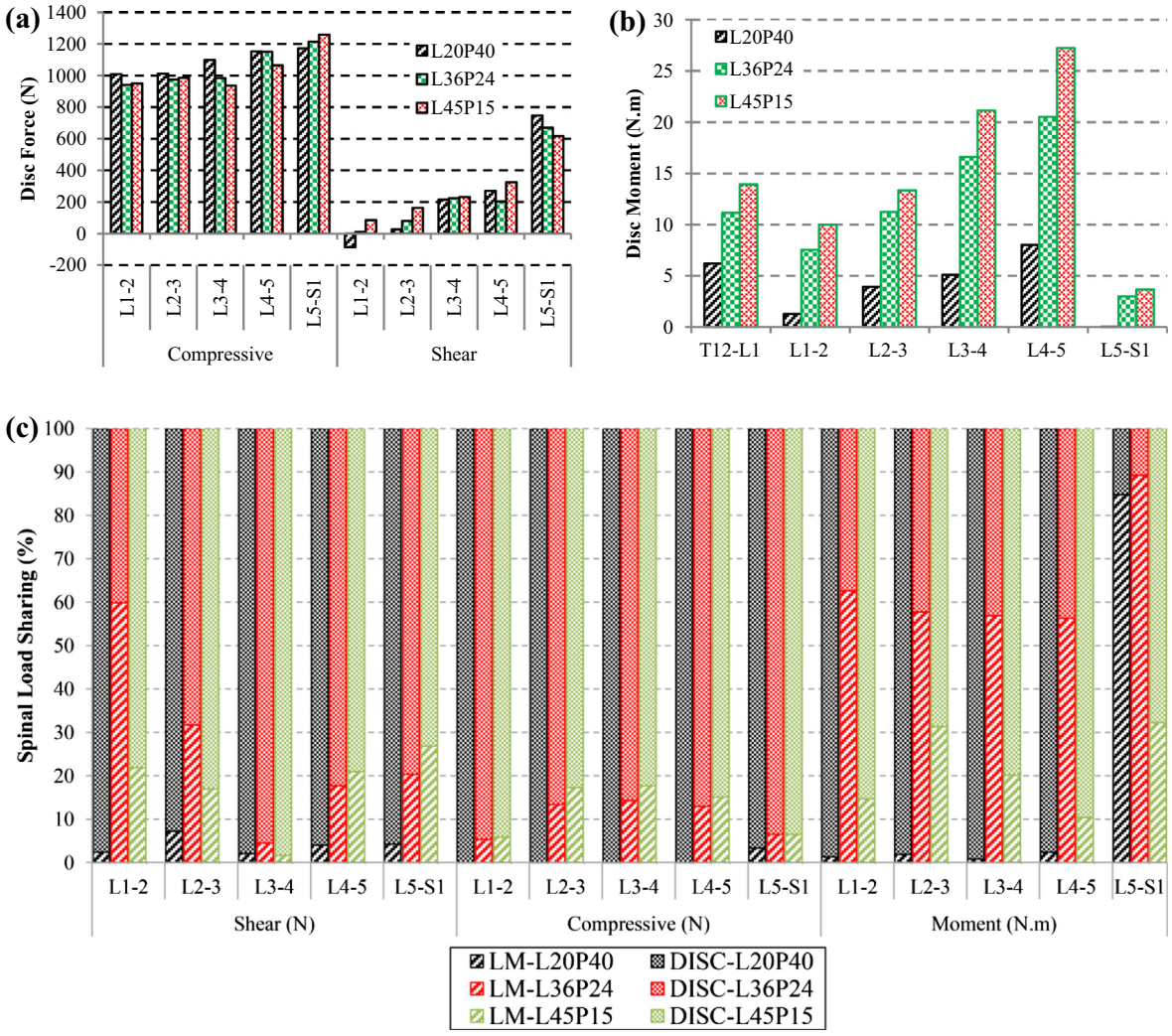

Fig. 7. Variation of disc internal forces (a) and moments (b) as well as load-sharing (c) with lumbo-pelvic rhythm at 60° trunk forward flexion (anterior shear force: +ve, sagittal moment: +ve in flexion, LM: ligament force, DISC: disc force, Facet joints have zero forces in all lumbo-pelvic rhythm cases).

The L20P40 model with high pelvic rotation produced the smallest disc moment while the greatest moment magnitude resulted from the rhythm with low pelvic rotation (model L45P15) (Fig. 7b). The maximum difference between these magnitudes reached ~20 Nm and occurred at the L4-5 level. The model with moderate pelvic rotation (L36P24) predicted disc moment values falling in between those predicted by the other models.

3.6. Load sharing

Load-sharing of a given spinal component is defined as percentage of the total spinal load carried by that component (Liu et al., 2018). In the L20P40 model (high pelvic rotation), shear, compression and moment were almost entirely carried by the discs alone except at the L5-S1 level where the ligaments contribution to moment resistance reached 85%. In the L36P24 model (moderate pelvic rotation), the disc had noticeable contribution to compressive and shear forces resistance as well while the ligaments contributed more to moment resistance, where their maximum moment-sharing reached 90% at the L5-S1 level. The force- and moment-sharing of the discs were also significant, as compared to the ligaments in case of the rhythm with low pelvic rotation. No contribution was observed for the facet joints in any of the three rhythms (Fig. 7c).

4. Discussion

Quantitative assessment of the lumbo-pelvic rhythm impact on key spinal biomechanics parameters provides valuable insight towards LBP treatment and disc injury prevention. This study investigated the effects of the lumbo-pelvic rhythm during moderate forward flexion on spinal response using a combined MSK and FE analysis approach. Three lumbo-pelvic rhythms with high, moderate, and low pelvic rotations were input into our previously validated MSK model in order to predict trunk muscle forces and joint reaction forces and moments for posture changing from upright to 60° forward flexion. The predicted forces and moments at 60° flexion were then applied to our previously validated FE model of a lumbosacral spine to predict the IDP, disc forces and moments, as well as load-sharing, and compare them in terms of the three lumbo-pelvic rhythms.

4.1. Muscle forces and disc loads

The observed influence of the lumbo-pelvic ratio on muscle forces was relatively small during initial flexion (<30°), but became increasingly larger when the flexion exceeded 30° particularly for the global muscles. The maximum difference in muscle forces predicted by the various lumbo-pelvic rhythms occurred at 60° flexion

and reached ~248N for the local muscles and ~83N for the global muscles. This is may be due to several factors including moment arms of the local muscles (Fig. 3) which are affected by the intervertebral rotation in the rhythm with high lumbar rotation and moment arms, or the global muscles which are influenced by the pelvic rotation in the rhythm with high pelvic rotation. The MF, LGPL, IO, EO, and QL muscles are attached to the vertebrae and pelvis (Fig. 1), and hence when the lumbar rotation increased (rhythm L45P15) the force in these muscles increased to ensure stability and balance the gravity forces. The ICPL, LGPT and ICPT muscles, attached to the thorax and sacrum (Fig. 1), generated greater forces when the rhythm involves high pelvic rotation. The optimization-based approach used in the current MSK model to estimate muscle forces predicted no force in the RA and PM muscles. Thus, the effects of the lumbo-pelvic rhythm on these muscles could not be quantified.

The lumbo-pelvic rhythm had less effect on the disc compressive and shear forces as compared to the moment. The variation in compression and shear is due to the variation in total (global + local) muscle force in the three rhythms, while the gravitational forces remained the same. However, the significant change in the disc moment is related to the lever arms of the gravity and muscle forces which changed with the lumbo-pelvic rhythm. Also, although the rhythms with moderate (L36P24) and high (L20P40) pelvic rotation have CoM with similar anterior location (i.e. similar lever arms for the gravitational forces), the former will have lower margin of stability as it had higher CoM (El-Rich and Shirazi-Adl, 2005). The rhythm that involves moderate pelvic and lumbar rotation (L36P24) is considered as normal rhythm adopted by asymptomatic individuals (Tafazzol et al., 2014), hence it produces disc loads that fall within those produced by the other rhythms and a balanced synergy between local and global muscles forces.

Tafazzol et al. (2014) measured the lumbo-pelvic ratios on eight young healthy males performing full flexion using inertia tracking device. They predicted the spinal loads for ratios varying from 0.5 to 3 with an interval of 0.25 using a MSK model. Their results revealed that the compressive and shear forces showed a maximum reduction of 21% and 45% respectively, at any specific trunk flexion angle when lumbo-pelvic ratio increases. In addition, effects of the lumbo-pelvic ratio on spinal forces at L5-S1 level become pronounced and exhibit a nonlinear pattern due to passive components when the trunk rotation increases. The shear force predicted in the current research follows similar trend, while the compressive shows opposite pattern at the L5-S1 level. This disagreement might be due to the difference in spine geometry used in both studies including lordosis, discs height, muscle architecture (number of muscles, insertion and attachment points).

4.2. IDP and annular fiber strain

The IDP at the L1-3 and L5-S1 levels was not affected by the lumbo-pelvic rhythm (Fig. 6) as the disc resultant force (compression and shear) was almost similar (~970N at L1-2, ~1000N at L2-3, ~1390N at L5-S1) in all cases. The IDP magnitude at the L4-5 level in all rhythm cases ranged from 1.6 MPa to 1.8 MPa which is slightly higher than the value obtained by interpolation (Azari et al., 2017) using the *in-vivo* data reported by Wilke et al. (2001). This is due to the disc cross sectional area which is smaller in our FE model than the one reported by Wilke et al. (2001) in addition to the difference in the upper body mass distribution and musculature.

Overall, the lumbo-pelvic rhythm affected the IDP, mainly at the L3-5 levels, where 50% of the total lumbar rotation was applied. The rhythm with high lumbar rotation increased the IDP particularly at the L3-5 levels, and shifted a proportion of the high tensile strain from the L5-S1 to the L3-5 levels. These effects, however, were relatively small as compared to the muscle forces and disc moment. In alignment with literature, the current research also confirms that using more pelvic motion relieves the IDP at L4-5 level (McClure et al., 1997). Our findings revealed that the lumbo-pelvic rhythm has little impact on IDP and annular fibers strain as compared to muscle forces and disc moment for moderate forward flexion ($\leq 60°$). These effects may become more pronounced for greater flexion angles.

4.3. Disc and ligament load-sharing

Our results revealed that the contribution of the discs and ligaments in load-bearing during forward flexion depends on the coordination between the lumbar spine and the pelvis, and that the facet joints have no contribution at all. For the same flexion angle (60°), a lumbo-pelvic rhythm with high pelvic rotation and low lumbar rotation increases the role of disc in resisting spinal forces and moments to reach 100% at some levels. By contrast, a rhythm that involves more lumbar rotation engages the ligaments to resist spinal load, particularly moments. A normal rhythm such as L36P24 with balanced (almost equal) pelvic and lumbar rotations yields almost equal disc and ligament load-sharing, confirming the well-established major role of the discs in load-bearing during forward flexion.

4.4. Methodological issues and limitations

Similar to other computational studies, the current research has assumptions and limitations. The spinal rhythm measured *in-vivo* by Granata and Sanford (2000) and used by Arjmand and Shirazi-Adl (2006) was considered by the MSK model and was kept constant during entire flexion for simplification. Future improvement requires continuous *in-vivo* measurement of the spinal rhythm and lumbo-pelvic rhythm during flexion. Once set, the lumbo-pelvic rhythms were also assumed constant during the simulation. The disc forces and moments were calculated based on equilibrium requirements at each level (Naserkhaki et al., 2016, Liu et al., 2018), where the FE model of the lumbosacral spine was subjected to the muscle forces, gravitational forces, and joint reaction forces and moments resulting from the upper body, as well as ligament forces at the T12-L1 level. The moments about points similar to the joint position in the MSK model (Liu et al., 2018) were calculated. Had the model considered different points such as the center of reaction (Ghezelbash et al., 2018), different magnitudes of disc moments would have been computed. The facet joint contact force in the MSK was determined by detecting the distance between contact points located on adjacent facet surfaces. However, the surface-to-surface contact is employed in the FE model to simulate facet joint interactions. Other limitations of the methodology are detailed elsewhere (Liu et al., 2018). In addition, although the influence of the lumbo-pelvic rhythm on muscle forces was quantified for posture changing from upright to 60° flexion, the disc loads, IDP, and load-sharing were determined at 60° flexion only as the effects of the lumbo-pelvic rhythm on muscle forces were maximum at this posture. This was also confirmed by the findings of Tafazzol et al. (2014). Thus, the predicted results are valid for moderate flexion only and cannot be generalized for large flexion.

Conclusion

In conclusion, the lumbo-pelvic rhythm during forward flexion has important effects on muscle forces and disc loads, as well as on load-sharing. However, less influence on the IDP and annular fibers strain was observed. In general, a rhythm with high pelvic rotation involves more global muscles, while more local muscles were

recruited in a rhythm with low pelvic rotation and high lumbar rotation. A normal rhythm yielded a more balanced synergy between global and local muscles and almost equal disc and ligament load-sharing. These findings improved knowledge on the spine biomechanics during forward flexion and are clinically relevant towards LBP treatment and disc injury prevention.

Conflicts of interest

The authors have no conflicts of interest concern.

Acknowledgement

This study is financially supported by the China Scholarship Council (201506080013) and NSERC Discovery Grant (402046-2013), Canada.

References

Arjmand, N., Plamondon, A., Shirazi-Adl, A., Larivière, C., Parnianpour, M., 2011. Predictive equations to estimate spinal loads in symmetric lifting tasks. J. Biomech. 44, 84–91. https://doi.org/10.1016/j.jbiomech.2010.08.028.

Arjmand, N., Shirazi-Adl, A., 2006. Model and in vivo studies on human trunk load partitioning and stability in isometric forward flexions. J. Biomech. 39, 510–521. https://doi.org/10.1016/j.jbiomech.2004.11.030.

Arshad, R., Zander, T., Dreischarf, M., Schmidt, H., 2016. Influence of lumbar spine rhythms and intra-abdominal pressure on spinal loads and trunk muscle forces during upper body inclination. Med. Eng. Phys. 38, 333–338. https://doi.org/10.1016/j.medengphy.2016.01.013.

Azari, F., Arjmand, N., Shirazi-Adl, A., Rahimi-Moghaddam, T., 2017. A combined passive and active musculoskeletal model study to estimate L4–L5 load sharing. J. Biomech., 1–9 https://doi.org/10.1016/j.jbiomech.2017.04.026.

Cholewicki, J., McGill, S.M., 1996. Mechanical stability of the in vivo lumbar spine: implications for injury and chronic low back pain. Clin. Biomech. 11, 1–15.

Damsgaard, M., Rasmussen, J., Christensen, S.T., Surma, E., de Zee, M., 2006. Analysis of musculoskeletal systems in the AnyBody Modeling System. Simul. Model. Pract. Theory 14, 1100–1111. https://doi.org/10.1016/j.simpat.2006.09.001.

de Zee, M., Hansen, L., Wong, C., Rasmussen, J., Simonsen, E.B., 2007. A generic detailed rigid-body lumbar spine model. J. Biomech. 40, 1219–1227. https://doi.org/10.1016/j.jbiomech.2006.05.030.

Dreischarf, M., Zander, T., Shirazi-Adl, A., Puttlitz, C.M., Adam, C.J., Chen, C.S., Goel, V. K., Kiapour, A., Kim, Y.H., Labus, K.M., Little, J.P., Park, W.M., Wang, Y.H., Wilke, H.J., Rohlmann, A., Schmidt, H., 2014. Comparison of eight published static finite element models of the intact lumbar spine: predictive power of models improves when combined together. J. Biomech. 47, 1757–1766. https://doi.org/10.1016/j.jbiomech.2014.04.002.

El-Rich, M., Shirazi-Adl, A., 2005. Effect of load position on muscle forces, internal loads and stability of the human spine in upright postures. Comput. Methods Biomech. Biomed. Eng. 8, 359–368. https://doi.org/10.1080/10255840500445630.

El-Rich, M., Arnoux, P.-J., Wagnac, E., Brunet, C., Aubin, C.-E., 2009. Finite element investigation of the loading rate effect on the spinal load-sharing changes under impact conditions. J. Biomech. 42, 1252–1262. https://doi.org/10.1016/j.jbiomech.2009.03.036.

Esola, M.A., McClure, P.W., Fitzgerald, G.K., Siegler, S., 1996. Analysis of lumbar spine and hip motion during forward bending in subjects with and without a history of low back pain. Spine 21, 71–78.

Fathallah, F.A., Marras, W.S., Parnianpour, M., 1999. Regression models for predicting peak and continuous three-dimensional spinal loads during symmetric and asymmetric lifting tasks. Hum. Factors 41, 373–388. https://doi.org/10.1518/001872099779611094.

Ghezelbash, F., Eskandari, A.H., Shirazi-Adl, A., Arjmand, N., El-Ouaaid, Z., Plamondon, A., 2018. Effects of motion segment simulation and joint positioning on spinal loads in trunk musculoskeletal models. J. Biomech. 70, 149–156. https://doi.org/10.1016/j.jbiomech.2017.07.014.

Granata, K.P., Sanford, A.H., 2000. Lumbar–pelvic coordination is influenced by lifting task parameters. Spine 25, 1413–1418.

Kim, M., Yi, C., Kwon, O., Cho, S., Cynn, H., Kim, Y., Hwang, S., Choi, B., Hong, J., Jung, D., 2013. Comparison of lumbopelvic rhythm and flexion-relaxation response between 2 different low back pain subtypes. Spine 38, 1260–1267.

Laird, R.A., Kent, P., Keating, J.L., 2016. How consistent are lordosis, range of movement and lumbo-pelvic rhythm in people with and without back pain? BMC Musculoskelet. Disord. 17. https://doi.org/10.1186/s12891-016-1250-1.

Liu, T., Khalaf, K., Naserkhaki, S., El-Rich, M., 2018. Load-sharing in the lumbosacral spine in neutral standing & flexed postures – A combined finite element and inverse static study. J. Biomech. 70, 43–50. https://doi.org/10.1016/j.jbiomech.2017.10.033.

McClure, P.W., Esola, M., Schreier, R., Siegler, S., 1997. Kinematic analysis of lumbar and hip motion while rising from a forward, flexed position in patients with and without a history of low back pain. Spine 22, 552–558.

Naserkhaki, S., Jaremko, J.L., Adeeb, S., El-Rich, M., 2016. On the load-sharing along the ligamentous lumbosacral spine in flexed and extended postures: finite element study. J. Biomech. 49, 974–982. https://doi.org/10.1016/j.jbiomech.2015.09.050.

Porter, J.L., Wilkinson, A., 1997. Lumbar-hip flexion motion. A comparative study between asymptomatic and chronic low back pain in 18- to 36-year-old men. Spine 22, 1508–1513. discussion 1513-1514.

Rohlmann, A., Neller, S., Claes, L., Bergmann, G., Wilke, H.-J., 2001. Influence of a follower load on intradiscal pressure and intersegmental rotation of the lumbar spine. Spine 26, E557–E561.

Rose, S.J., Sahrmann, S.A., Norton, B.T., 1988. Quantitative assessment of lumbar-pelvic rhythm. Phys. Ther. 68, 824.

Schmidt, H., Heuer, F., Simon, U., Kettler, A., Rohlmann, A., Claes, L., Wilke, H.-J., 2006. Application of a new calibration method for a three-dimensional finite element model of a human lumbar annulus fibrosus. Clin. Biomech. 21, 337–344. https://doi.org/10.1016/j.clinbiomech.2005.12.001.

Schmidt, H., Kettler, A., Heuer, F., Simon, U., Claes, L., Wilke, H.-J., 2007. Intradiscal pressure, shear strain, and fiber strain in the intervertebral disc under combined loading. Spine 32, 748–755.

Tafazzol, A., Arjmand, N., Shirazi-Adl, A., Parnianpour, M., 2014. Lumbopelvic rhythm during forward and backward sagittal trunk rotations: combined in vivo measurement with inertial tracking device and biomechanical modeling. Clin. Biomech. 29, 7–13. https://doi.org/10.1016/j.clinbiomech.2013.10.021.

Vazirian, M., Van Dillen, L.R., Bazrgari, B., 2016. Lumbopelvic rhythm in the sagittal plane: a review of the effects of participants and task characteristics. Int. Musculoskelet. Med. 38, 51–58. https://doi.org/10.1080/17536146.2016.1241525.

Wilke, H., Neef, P., Hinz, B., Seidel, H., Claes, L., 2001. Intradiscal pressure together with anthropometric data–a data set for the validation of models. Clin. Biomech. 16 (Suppl 1), S111–S126.